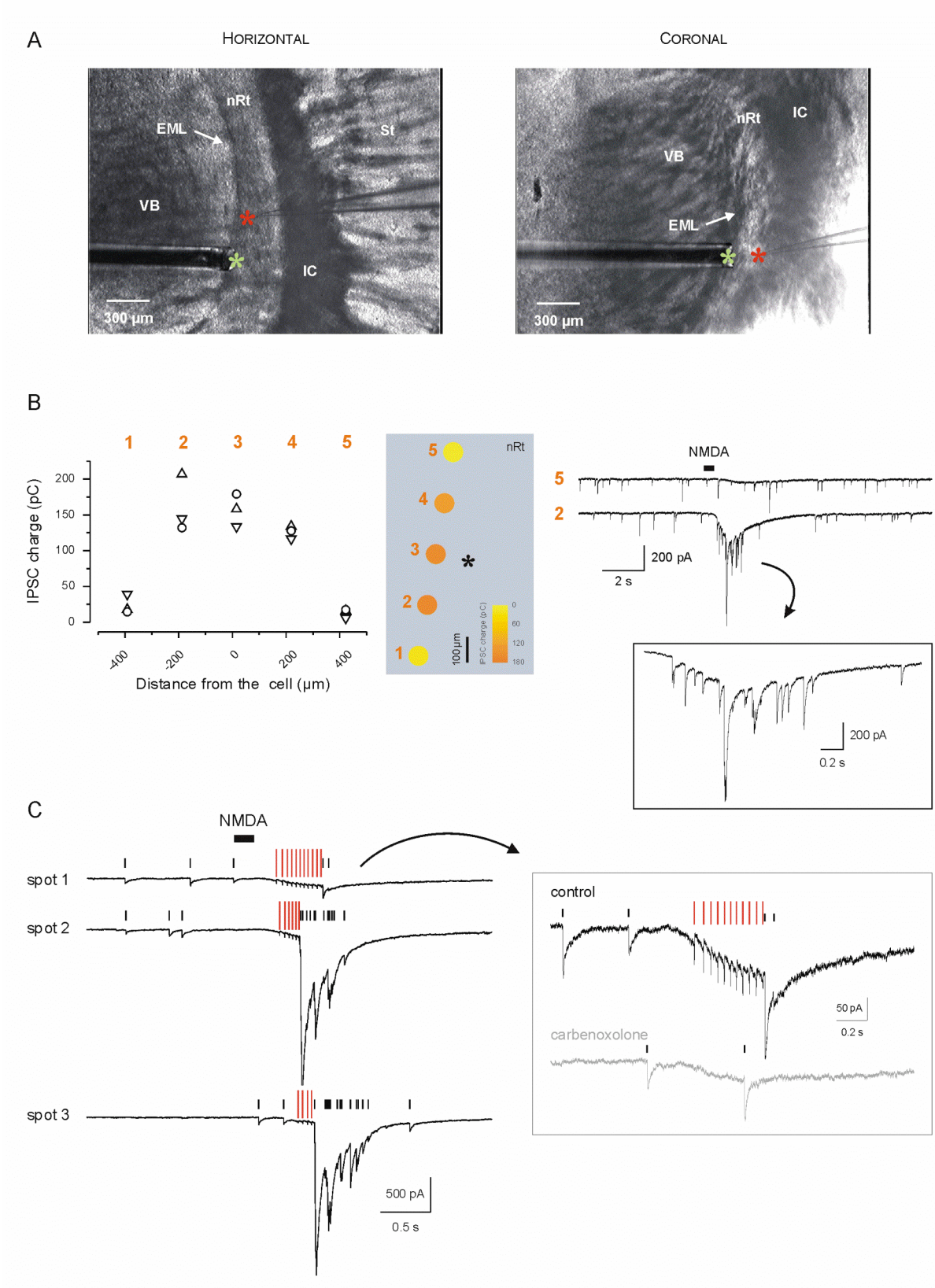

Supplemental Figure 1

Supplemental Figure 1. *Mapping of intra-nRt connectivity at coarse resolution. Methods*: Whole-cell recordings were obtained in voltage clamp mode at -60 mV, using an intracellular solutions containing (in mM): 130 CsCl, 10 Hepes, 10 EGTA, 5 QX-314, 2 Mg-ATP, 0.3 Na-GTP (E_{Cl} ~ -1 mV). A mix of NMDA (0.5 mM) and glycine (5 μM) was applied for 100-500 ms using a precise local (I.D. 100 μm) perfusion system that delivered the excitatory stimulus at an angle normal to the long axis of the nRt, thus activating a large group of cells along the mediolateral extent of the nucleus. Under these conditions robust inhibitory synaptic output and rebound burst firing occurred in relay neurons and was detected as late EPSCs in the recorded nRt cell (not shown). Thus we blocked AMPA receptors with 10 μM NBQX, and accordingly fast recurrent excitation that could potentially recruit ectopic nRt cell activation, which would compromise interpretation of the map. Slow, small recurrent NMDA receptor mediated EPSPs were triggered in nRt cells by these stimuli or by direct application of NMDA into VB, but these were insufficient to trigger action potentials (not shown, n=10). [Similar stimuli applied to VB in absence of NBQX did induce nRt cell firing (not shown, n=3)]. Our PSC detection criteria (primarily a rise time <2 ms) ensured that NMDA dependent EPSCs did not contaminate the IPSC maps. The aCSF contained 1 mM $MgCl_2$ in these experiments to decrease the Mg^{2+} block of NMDA receptors. The movement of the local perfusion delivery pipe was controlled by the same robotic system as described in the *Methods* section for the laser scanning photostimulation, but using a linear pattern of stimulation with 100-200 μm spacing between adjacent positions and a 20 seconds interval. Recordings were analyzed during the pre-stimulus (4 sec), triggered (4 sec) and post-stimulus (4 sec) period. *A*, Low power videomicroscopic images of horizontal and coronal thalamic slices. The local perfusion tubing (green asterisk) was always oriented perpendicular to the transverse axis of nRt to minimize the width of nRt activation, and towards the striatum (St) to avoid diffusion of NMDA to the ventrobasal complex (VB). The tip was moved at regular intervals along the external medullary lamina (EML) to encompass a region extending ~ 500 μm on either side of the recorded cell (red asterisk). *B*, Representative example of IPSCs evoked by NMDA applied in multiple trials at five different locations (1 through 5). The net IPSC charge elicited at each site was calculated using the following equation: *total IPSC charge during the triggered period - (sum of total IPSC charge during the pre and post period ÷ 2)* to account for spontaneous activity, and plotted as a function of the distance between the local perfusion tip and the recorded cell. Total charge was calculated as number of events × mean peak

IPSC × IPSC weighted decay time constant. IPSCs are inward under these conditions. Three successive trials were obtained (each with a different symbol), and the averaged values represented on a map using a color scale, the asterisk indicating the location of the recorded cell. As illustrated in the example traces, NMDA applied close to the postsynaptic cell (site 2) triggered a barrage of large IPSCs on a top of a slow depolarization with the latter reflecting the direct activation, whereas at a more distant site (site 5) no increase in synaptic responses above a spontaneous baseline rate were detected. *C*, In some cells, NMDA triggered IPSCs as well as small and fast depolarizing currents identified as spikelets. The latter were presumably mediated by electrical coupling between the pre and postsynaptic cells, as they were abolished by 100 μM carbenoxolone, a gap junction blocker (inset, n=4 cells), while IPSCs were not. Different numbers and types of each event were triggered at each spot, indicating distinct maps for chemical vs electrotonic connectivity. Spots 1, 2, 3 were located at +69, -58, -184 μm from the recorded cell, respectively. Black and red bars represented above each traces indicate detected IPSCs and spikelets, respectively.

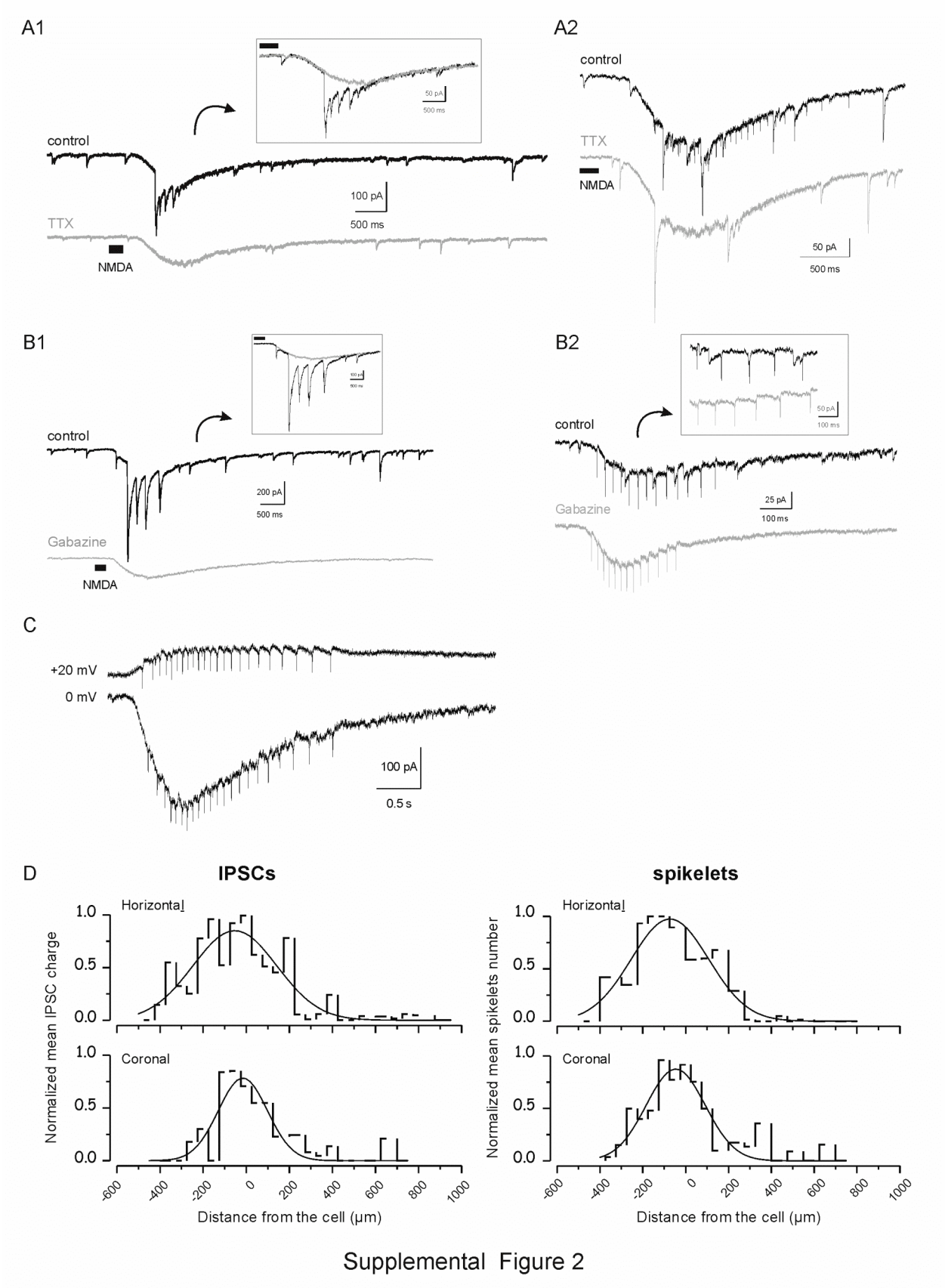

Supplemental Figure 2

Supplemental Figure 2. *Characterization of the response types and maps obtained with local perfusion.* *A*, The addition of TTX in the bath solution to block voltage dependent Na^+ channels, completely abolished both evoked IPSCs (A1, A2, n=2) and spikelets (A2, n=2), while the direct NMDA induced inward current (n=5) and miniature spontaneous IPSCs (n=7) remained intact. This result indicates that the 2 types of synaptic responses evoked by NMDA are dependent on the generation of action potentials in presynaptic cells. *B*, The $GABA_A$ receptors antagonist, gabazine (10 μM), blocked spontaneous (n=20) and evoked IPSCs (n=2, e.g. B1, B2) but didn't affect spikelets (n=2, e.g. B2), indicating that IPSCs, but not spikelets were mediated via $GABA_A$ receptors. *C*, Depolarization of the postsynaptic cell inverted the NMDA dependent direct current response from inward to outward, but did not affect the small and fast spikelets, which remained inward and whose amplitudes were generally unaffected by the membrane potential. *D*, One dimensional synaptic maps indicating the extent of connectivity along the long axis of nRt. Mapped are normalized net evoked IPSC charge and number of spikelets as a function of distance from the recorded cell. The data are fitted with a Gaussian function providing an estimation of width of connectivity. The extent of IPSC connectivity was larger in horizontal sections (390 ± 42, n=13 in horizontal vs 228 ± 22, n=13 in coronal). The same trend was observed with electrical coupling (362 ± 30, n=9 in horizontal vs 275 ± 31, n=13 in coronal). We observed electrical synaptic responses in 13 of 28 neurons (46%) in coronal slices and 9 of 24 neurons (38%) in horizontal slices, and chemical synaptic responses in 13 of 28 neurons (46%) in coronal slices and 13 of 24 neurons (54%) in horizontal slices. 29% of cells (8/28) in coronal slices were connected exclusively via electrical synapses vs 13% of cells (3/24) in horizontal slices.